

# Specific expression and methylation of *SLIT1*, *SLIT2*, *SLIT3*, and miR-218 in gastric cancer subtypes

MIRANG KIM<sup>1,2</sup>, JONG-HWAN KIM<sup>1,2</sup>, SU-JIN BAEK<sup>1,2</sup>, SEON-YOUNG KIM<sup>1,2</sup> and YONG SUNG KIM<sup>1,2</sup>

<sup>1</sup>Genome Research Center, Korea Research Institute of Bioscience and Biotechnology (KRIBB);

<sup>2</sup>Department of Functional Genomics, University of Science and Technology, Daejeon 34141, Republic of Korea

Received December 20, 2015; Accepted January 27, 2016

DOI: 10.3892/ijo.2016.3473

**Abstract.** SLIT has been suggested as a key regulator of cancer development and a promising therapeutic target for cancer treatment. Herein, we analyzed expression and methylation of *SLIT1/SLIT2/SLIT3* in 11 gastric cancer cell lines, 96 paired gastric tumors and adjacent normal gastric tissues, and 250 gastric cancers provided by The Cancer Genome Atlas. Methylation of *SLIT1/SLIT2/SLIT3* was found both in early gastric cancers, and in advanced gastric cancers. Even normal gastric tissue showed increased methylation of *SLIT1* and *SLIT3* that correlated with patient age. Furthermore, epigenetic inactivation of *SLIT* occurred in a gastric cancer subtype-dependent manner. *SLIT2* and *SLIT3* expression was reduced in Epstein-Barr virus-positive and microsatellite instability subtypes, but increased in the genomically stable subtype. Expression of miR-218 correlated negatively with methylation of *SLIT2* or *SLIT3*. These findings suggest that a molecular subtype-specific therapeutic strategy is needed for targeting SLITs and miR-218 in treatment of gastric cancer.

## Introduction

Gastric cancer is a heterogeneous disease that has its basis in various genetic and epigenetic alterations. Based on Lauren's classification, gastric cancer has been divided into two histological subtypes, namely the intestinal type and diffuse type (1). Recent advances in high-throughput analysis have delivered new insights into the heterogeneity underlying distinct molecular subtypes of gastric cancer. The Cancer Genome Atlas (TCGA) network investigated exome sequences, copy-number alterations, gene expression, DNA methylation, and protein activities of gastric cancers and classified gastric cancers into four subtypes: Epstein-Barr virus (EBV)-positive,

microsatellite instability (MSI), genomically stable (GS), and chromosomal instability (CIN) (2). Nearly 9% of gastric cancer is EBV-positive (3), for which methylation of tumor suppressor genes is a key abnormality (4). MSI is a common feature of gastric cancers that occurs in 15-30% of cases (5). DNA mismatch repair deficiency such as methylation of the *MLH1* promoter increases the frequency of mutations across the genome, creating MSI (5). Not only *MLH1* but also many other tumor suppressor genes are frequently hypermethylated in MSI-positive gastric cancer (6). The GS subtype is characterized by the enrichment of diffuse-type gastric cancer, which is an aggressive, invasive, and stem-like histological subtype (2). This molecular classification has important biological and clinical implications for basic research, diagnosis, and drug treatment of gastric cancer.

SLIT proteins are highly conserved secreted glycoproteins and the main ligands for roundabout receptors (ROBOs) (7). The SLIT/ROBO pathway plays an important part in cell-signaling pathways including axon guidance, cell migration, cell motility, and angiogenesis. Recent studies indicate that SLIT proteins have important roles in tumorigenesis, cancer progression, and metastasis (8,9). Three genes encoding SLITs (*SLIT1*, *SLIT2* and *SLIT3*) have been characterized in mammals. *SLIT1* is located on human chromosome 10q24.1, *SLIT2* is on 4p15.31, and *SLIT3* is on 5q34-q35.1. *SLIT2* regulates the  $\beta$ -catenin/TCF and PI3K/AKT signaling pathways and enhances cell-cell adhesion in breast cancer (10). Knockdown of *SLIT2* promotes gastric cancer cell proliferation and migration via activation of AKT/ $\beta$ -catenin signaling (11). *SLIT2* and *SLIT3* are frequently methylated and down-regulated in various cancers such as breast (12), colorectal (13), cervical (14), and lung (12), but their methylation status in gastric cancer has not been unequivocally defined.

miR-218 is an intronic microRNA (miRNA) co-expressed with its host genes, *SLIT2* and *SLIT3* (15). The mature form of miR-218 is generated from two separate loci, *miR-128-1* and *miR-218-2*, which are located within the introns of *SLIT2* and *SLIT3*, respectively (16). miR-218 functions as a tumor suppressor, inhibiting cell invasion and metastasis (17). In gastric cancer cells deficient in miR-218 expression, ectopic expression of miR-218 suppresses both ROBO1 expression and tumor cell invasiveness/metastasis (18).

The genome-wide DNA methylation profiling of gastric cancer reported here shows that the CpG islands of *SLIT1*,

---

Correspondence to: Dr Yong Sung Kim, Genome Research Center, Korea Research Institute of Bioscience and Biotechnology (KRIBB), 125 Gwahak-ro, Yuseong-gu, Daejeon 34141, Republic of Korea  
E-mail: yongsung@kribb.re.kr

**Key words:** SLIT1, SLIT2, SLIT3, miR-218, methylation, gastric cancer

*SLIT2* and *SLIT3* are hypermethylated. We analyzed expression and methylation of *SLITs* in gastric cancer cell lines and primary gastric tumors. We also analyzed subtype-specific methylation and expression of *SLITs* using TCGA data. Furthermore, we examined the correlation between miR-218 expression and CpG island methylation of *SLIT2* or *SLIT3* in gastric cancer.

## Materials and methods

**Cell lines and tissue samples.** Eleven gastric cancer cell lines were obtained from the Korean Cell Line Bank and were cultured in RPMI-1640 supplemented with 10% fetal bovine serum and 1% antibiotic-antimycotic solution (Invitrogen, Carlsbad, CA, USA). Ninety-six paired frozen gastric tumor tissues and normal adjacent tissues were collected from the Tissue Bank at Chungnam National University Hospital. All samples were obtained with informed consent, and their use was approved by the institutional review board (19).

**Methylated DNA-binding domain sequencing (MBD-seq).** MBD-seq was performed as described (20). Briefly, methylated DNA was precipitated from 1  $\mu$ g of fragmented genomic DNA via binding to the methyl-CpG-binding domain of human MBD2 protein using the MethylMiner methylated DNA enrichment kit (Invitrogen). The methylated DNA fragments were ligated to a pair of adaptors for sequencing on the Illumina HiSeq 2500 sequencing system. The ligation products were size fractionated to obtain 250-350-bp fragments on a 2% agarose gel and subjected to 18 cycles of PCR amplification. Cluster generation and 100 cycles of paired-read sequencing were done. The sequences were mapped to the human genome (UCSC hg19). The sequencing data have been deposited in the NCBI Gene Expression Omnibus (GEO) under accession no. GSE46595.

**Quantitative reverse transcription (qRT)-PCR.** qRT-PCR was performed as described (21). RNA was isolated using the RNeasy kit (Qiagen, Valencia, CA, USA) and treated with DNase I (Promega, Madison, WI, USA). Total RNA (5  $\mu$ g) was reverse-transcribed into cDNA using SuperScript II (Invitrogen). qRT-PCR was done in a Bio-Rad CFX96 real-time PCR detection system (Bio-Rad, Foster City, CA, USA). cDNA (100 ng) was amplified in a 15- $\mu$ l reaction containing 2X SYBR Premix EX Taq (Takara, Shiga, Japan) using the primer sets listed in Table I. Samples were heated to 95°C for 30 sec, followed by 39 cycles of 95°C for 30 sec, 60°C for 30 sec, and 72°C for 30 sec. The gene encoding  $\beta$ -actin was used as an internal control. Each expression level was expressed as the cycle threshold (CT) value, and the difference in CT values for the gene and  $\beta$ -actin was calculated. Each mRNA level in tumors is presented relative to that of the normal tissue counterpart. If the expression level in the tumor was less than half that in paired normal tissue, it was considered a 'loss of expression'.

**Methylation-specific PCR (MSP).** MSP was performed as described (22). Genomic DNA was modified by sodium bisulfite using the Ez DNA Methylation kit (Zymo Research, Orange, CA, USA). Bisulfite-modified DNA (50 ng) was

amplified in a 20- $\mu$ l reaction with primers specific for methylated DNA (Table I) as follows: 94°C for 5 min, 35 cycles of 94°C for 30 sec, at the given annealing temperature for 30 sec, and 72°C for 60 sec, followed by 72°C for 10 min. The PCR products were separated on a 3% agarose gel and visualized with ethidium bromide staining.

**Pyrosequencing.** Methylation was quantified by pyrosequencing at selected CpG sites in *SLIT* genes. For *SLIT1*, CpG sites at 99, 107, 110, 112, 114, 122, and 124 bases from the transcription start site (TSS) were analyzed. For *SLIT2*, CpG sites at -1,489, -1,486, -1,478, -1,472, -1,466, -1,460, -1,458, and -1,453 bases from the TSS were analyzed. For *SLIT3*, CpG sites at 77, 80, 83, 86, 90, 95, and 100 bases from the TSS were analyzed. Pyrosequencing was performed as described (19) using primers listed in Table I. Bisulfite-modified DNA (100 ng) was used in a 25- $\mu$ l reaction containing the primer set and 2X Premix EX Taq (Takara). All samples were heated to 95°C for 5 min and then amplified for 50 cycles of 95°C for 30 sec, 60°C for 40 sec, and 72°C for 30 sec, followed by a final extension step at 72°C for 5 min. Pyrosequencing reactions were carried out using a sequencing primer and the PSQ HS 96A System (Biotage, Uppsala, Sweden) according to the specifications of Biotage.

**5-Aza-2'-deoxycytidine (5-Aza-dC) treatment.** The two gastric cancer cells SNU-601 and SNU-638 were seeded at a density of  $1 \times 10^6$  cells/10-cm dish 1 day before drug treatment. The cells were treated with 10  $\mu$ M 5-Aza-dC (Sigma, St. Louis, MO, USA) every 24 h for 3 days and then harvested. Total RNA was prepared for each cell sample, and changes in *SLIT* expression were measured by qRT-PCR as described above.

**Statistical analysis.** The significance of differences in CpG region hypermethylation between normal and tumor tissues was inferred using the paired t-test. The correlation between downregulation of *SLITs* and hypermethylation of *SLIT* CpG regions was inferred from the Pearson's correlation test. A linear model was used to understand the contribution of each clinical variable to the observed differences in *SLIT* expression and promoter hypermethylation. Six clinical parameters were used: tumor (tumor vs. normal), tumor depth (early vs. advanced gastric cancer), age, gender, TNM stage (IA, IB, II, IIIA, IIIB and IV), and Lauren's classification (intestinal vs. diffuse). The model formula was *SLIT* - tumor + histology + depth + age + gender + stage + Lauren. The R statistical language (<http://cran.r-project.org>) was used for all statistical tests. To compare characteristics of the different groups of patients, the t-test and analysis of variance were used. A p-value <0.05 was considered significant.

## Results

**Methylation of CpG islands in *SLIT1*, *SLIT2* and *SLIT3* in gastric cancer.** To identify differentially methylated genes in gastric cancer, we performed MBD-seq, a high-throughput sequencing of methylated DNA fragments captured by methyl-CpG-binding domain protein 2, of patient-derived gastric cancer cells and adjacent normal gastric mucosa cells. Among the differentially methylated regions, we found that

Table I. Primers for RT-PCR, MSP, and pyrosequencing.

Primers for RT-PCR					
Gene	Forward primer (5'-3')	Reverse primer (5'-3')	Annealing temperature (°C)	Product size (bp)	
<i>SLIT1</i>	CTGGTTGCCTTTGACCAGAT	TGTACAGGTTTCGGATGCAA	60	205	
<i>SLIT2</i>	TCAAGGTCCTGTGGATGTCA	GTGGCAAGTTCCTCCATGTT	60	199	
<i>SLIT3</i>	CCTGCCCTACAGCTACAAG	TTGTTTTCGCAGTCGTTGTC	60	199	
Primers for MSP					
Gene	Forward primer (5'-3')	Reverse primer (5'-3')	Annealing temperature (°C)	Product size (bp)	
<i>SLIT1</i>	AATTAAGAATTGATATAGCGAGTCG	ACACACACGACGAAAATACG	57	197	
<i>SLIT2</i>	GTAGAGCGTCGTTAAGGACGT	CGAAAATAAAAAACGCGAA	58	284	
<i>SLIT3</i>	AATGGAGAGAGCGAGCGTC	AACCCGCGAACCGAATTA	60	149	
Primers for pyrosequencing					
Gene	Forward primer (5'-3')	Reverse primer (5'-3')	Sequencing primer (5'-3')	Annealing temperature (°C)	Product size (bp)
<i>SLIT1</i>	TGGAGGAGTAAGGTGTTTTTAG	Biotin-ATCAACCCATAATACCTC	GAGTAAGGTGTTTTTAGTT	60	170
<i>SLIT2</i>	TAAGGAGGGAGTGTTGAGTAGAAA	Biotin-ACTCCCAAACCCCTAACAAAT	TGTTGAGTAGAAAGGGGA	60	212
<i>SLIT3</i>	GGGGGAGTTTAGTATTTGGGTAT	Biotin-CCACCCCAAACCCATAATATA	GGTTTAGTAGATGGAGTTG	60	282

CpG islands in *SLITs* were hypermethylated in gastric cancer (Fig. 1A). To examine the relationship between expression and methylation of *SLITs* in gastric cancer, we analyzed the expression of *SLITs* in gastric cancer cell lines using RT-PCR and methylation status using MSP. *SLIT1* was repressed in 55% (6 of 11) of gastric cancer lines, *SLIT2* was repressed in 73% (8 of 11), and *SLIT3* was repressed in 82% (9 of 11) (Fig. 1B). The inactivation of *SLITs* correlated with CpG island methylation as revealed by MSP (Fig. 1B). To assess DNA methylation at single-base resolution, we also performed pyrosequencing (Fig. 1C). The gastric cancer cell line SNU-601 had heavily methylated CpG sites of *SLITs*, but SNU-668 cells showed hypomethylation. In addition, these CpG sites were hypomethylated in normal tissues and moderately methylated in tumors (Fig. 1C). We next treated SNU-601 and SNU-638 cells with the DNA methylation inhibitor 5-Aza-dC (23) to examine whether the silencing of *SLITs* in gastric cancer cells could be reversed. Treatment with 5-Aza-dC induced the expression of *SLITs* (Fig. 1D), suggesting that DNA methylation plays a causal role in *SLIT* silencing in gastric cancer cells.

**Downregulation of *SLITs* in primary gastric tumors by CpG island methylation.** We next used qRT-PCR to assess *SLIT* expression in 96 paired normal and gastric tumor tissues. Data could not be obtained for five tissue pairs for *SLIT1* and one tissue pair for *SLIT3*, so they were omitted from this analysis. Expression of *SLIT1*, *SLIT2* and *SLIT3* was significantly reduced in tumors (Fig. 2A). Loss of expression, defined as tumor-specific expression >2-fold lower compared with normal

tissue, was observed in 76.9% (70 of 91), 63.2% (60 of 95), and 72.9% (70 of 96) of tumors for *SLIT1*, *SLIT2* and *SLIT3*, respectively. We also measured the methylation levels of *SLITs* in paired normal and tumor DNAs by pyrosequencing. Among 96 paired normal and tumor tissues used in qRT-PCR, 83 paired DNAs were available for this analysis. One tissue pair for *SLIT1*, four tissue pairs for *SLIT2*, and five tissue pairs for *SLIT3* were omitted from the analysis because of poor data generation. Tumor DNAs showed a significant methylation increase of 2.3-fold for *SLIT1*, 2.9-fold for *SLIT2*, and 1.5-fold for *SLIT3* compared with normal tissues (Fig. 2B,  $p < 0.0001$ ). Regression analysis showed that decreased *SLIT* expression correlated with increased CpG methylation (Fig. 2C-E). The correlation was highly significant for *SLIT2* ( $r = -0.3111$ ,  $p = 0.0056$ ) and *SLIT3* ( $r = -0.3531$ ,  $p = 0.0015$ ) but not significant for *SLIT1* ( $r = -0.1844$ ,  $p = 0.1082$ ).

**Methylation status of *SLITs* during gastric carcinogenesis and aging.** Inactivation of *SLITs* occurred in early-stage as well as in advanced-stage tumors and in both intestinal type and diffuse type (Fig. 3). As expected, based *SLIT* expression patterns, methylation of *SLITs* occurred in early-stage and advanced-stage tumors, and both intestinal-type and diffuse-type tumors showed high levels of methylation (Fig. 3). Although no clinical parameter was significantly related to *SLIT* methylation, we observed a positive correlation of a gradual increase of methylation status with increasing patient age (Fig. 4). Regression analysis revealed a significant correlation for *SLIT1* (Fig. 4A,  $p = 0.0067$ ) and *SLIT3* (Fig. 4C,

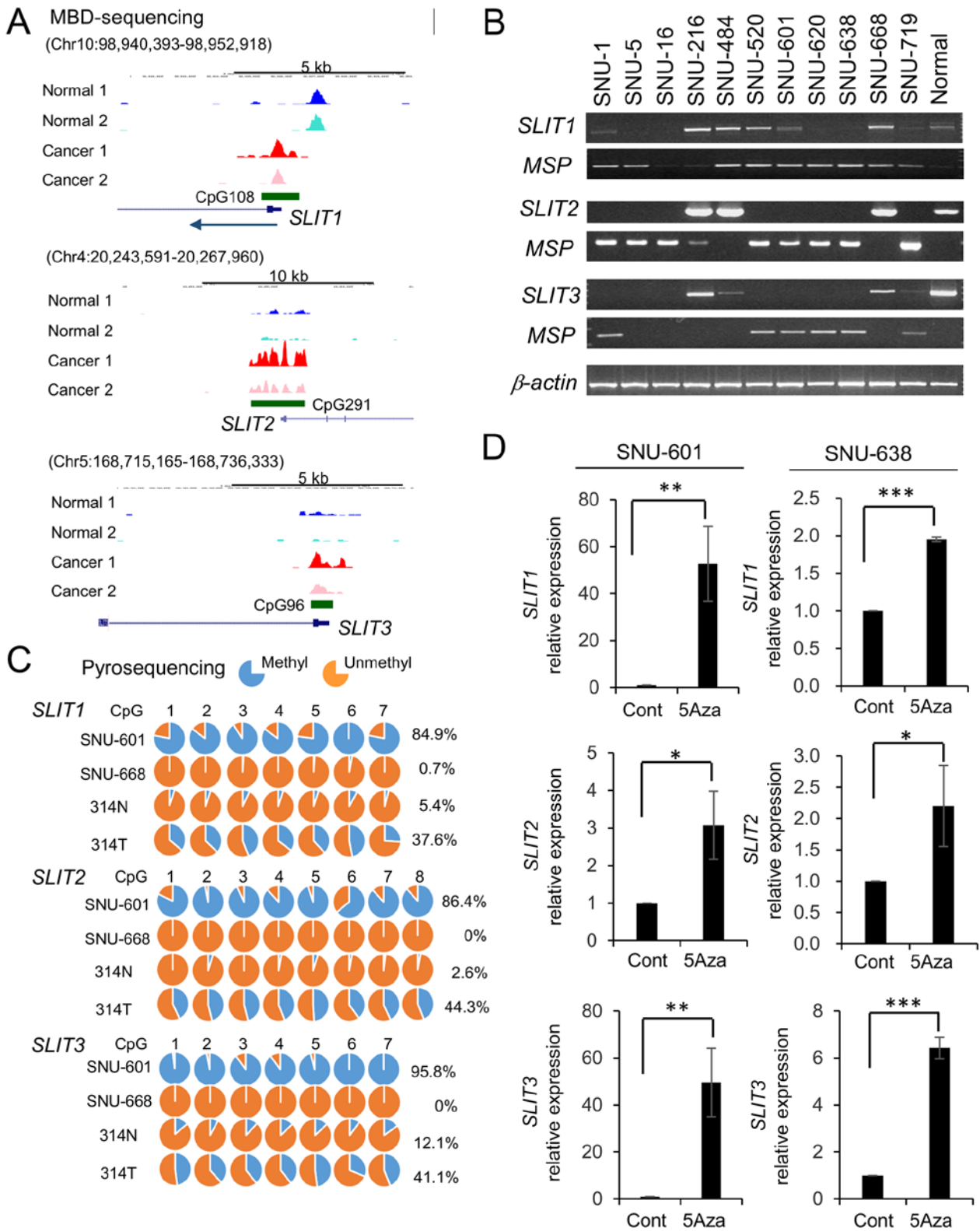


Figure 1. CpG island methylation of *SLIT1*, *SLIT2* and *SLIT3* in gastric cancer. (A) MBD-seq data for 5' CpG islands of *SLIT1*, *SLIT2* and *SLIT3* in patient-derived gastric cancer cells and adjacent normal gastric mucosa cells. (B) RT-PCR and MSP of *SLITs* in 11 gastric cancer cell lines and normal gastric tissue. (C) Pyrosequencing analysis of *SLITs* in SNU-601, SNU-668, and paired gastric tumor (314T) and adjacent normal tissue (314N). Mean methylation for each analysis is presented as the percentage on the right. (D) Reactivation of *SLITs* after treatment with 5-Aza-dC (5Aza) (mean  $\pm$  standard error, \* $p$ <0.05, \*\* $p$ <0.01, \*\*\* $p$ <0.001).

$p=0.0011$ ) but not for *SLIT2* (Fig. 4B,  $p=0.1064$ ) in normal tissues. The positive correlation was also observed in tumor tissues, but the significance was maintained only for *SLIT3*

(Fig. 4F,  $p=0.0078$ ). These data suggested that *SLIT3* is methylated in both an age- and cancer-related manner, but *SLIT2* is methylated only in a cancer-related manner.

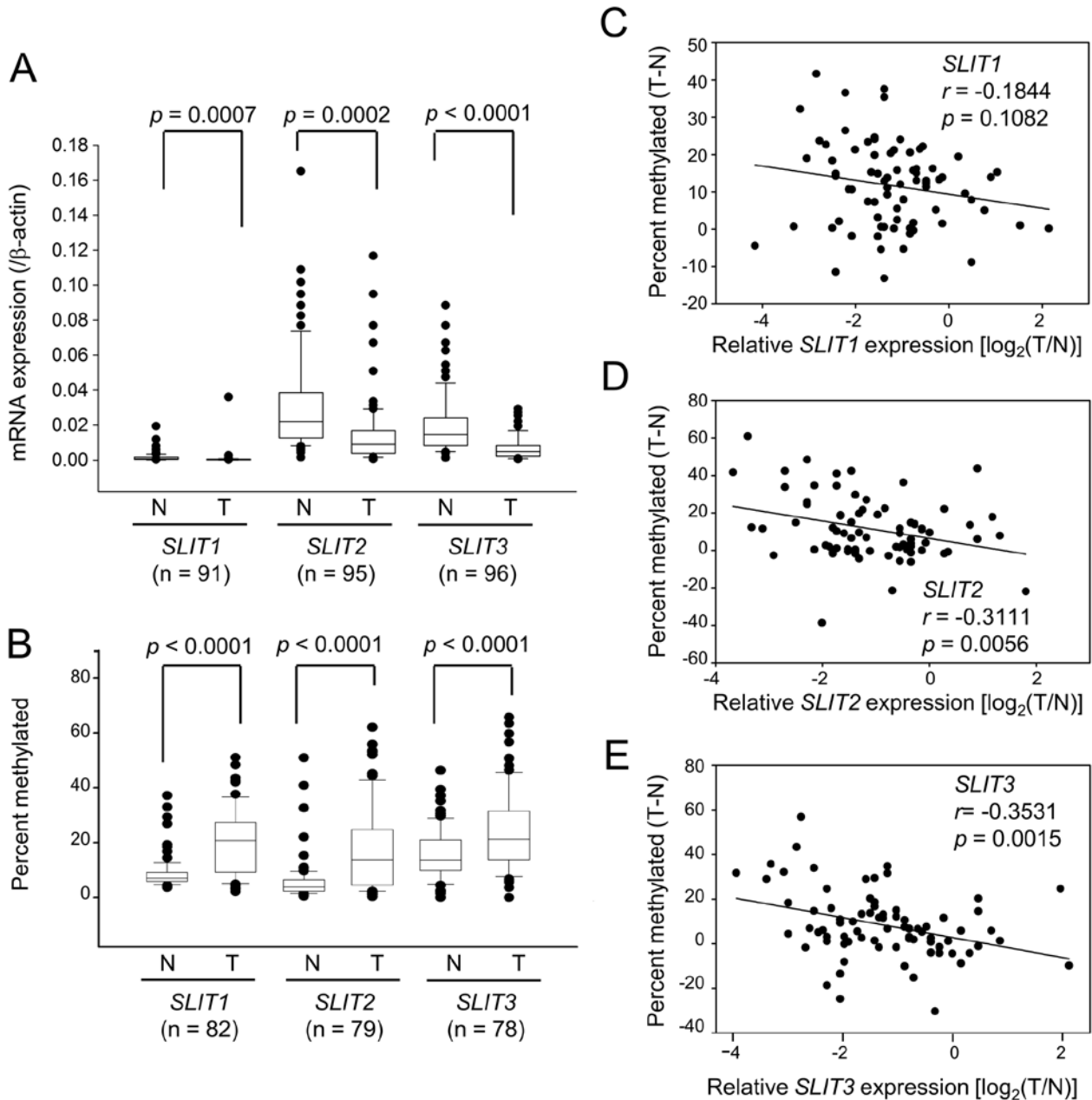


Figure 2. Expression and methylation of *SLIT1*, *SLIT2* and *SLIT3* in primary gastric tumors. (A) *SLIT* mRNA expression, relative to that of  $\beta$ -actin, in the paired gastric normal and tumor tissues. The statistical significance of differential expression between normal and tumor tissues was inferred using the paired t-test. Each box plot shows the median and 25th and 75th percentiles, and the dots represent outliers. (B) Methylation of *SLITs* in the paired gastric normal and tumor tissues. Pyrosequencing analysis was performed at the seven (*SLIT1*, *SLIT3*) or eight (*SLIT2*) CpG sites of the CpG islands. The statistical significance of differential methylation between normal and tumor tissues was inferred using the paired t-test. (C-E) The relationship between *SLIT* expression and methylation of *SLIT1* (C), *SLIT2* (D), and *SLIT3* (E). This analysis was performed with clinical samples for both expression and methylation data. The methylation change is expressed as the difference between paired tumor and normal tissues (T-N). Expression values are expressed as the  $\log_2$  ratio of tumor samples over normal samples.

#### Subtype-specific expression and methylation status of *SLITs*.

To elucidate the specific expression and methylation status of *SLITs* in gastric cancer subtypes (EBV-positive, MSI, GS, and CIN), we analyzed RNA-seq data and Infinium 450K methylation array data for gastric cancers provided by TCGA (2). TCGA provides methylation array data for 250 gastric tumor samples but only 2 normal samples, so we collected other public data for 10 normal gastric tissue samples (24,25) and data for 1 sample in our laboratory. Fig. 4 shows the methylation profile of the 13 normal gastric tissues and 25 EBV,

51 MSI, 52 GS, and 122 CIN subtype gastric cancer tissues in the *SLIT1* CpG island (13 CpG sites), *SLIT2* CpG island (12 sites), and *SLIT3* CpG island (10 sites). *SLIT1*, *SLIT2* and *SLIT3* showed similar subtype-dependent methylation patterns (Fig. 5). As expected, the EBV-positive and MSI subtypes had high levels of DNA methylation in the *SLIT* CpG islands. Although the GS subtype had higher *SLIT* methylation levels than normal gastric tissue, the methylation differences were slight. The CIN subtype showed a broad range of methylation levels of *SLITs* promoters (Fig. 5).

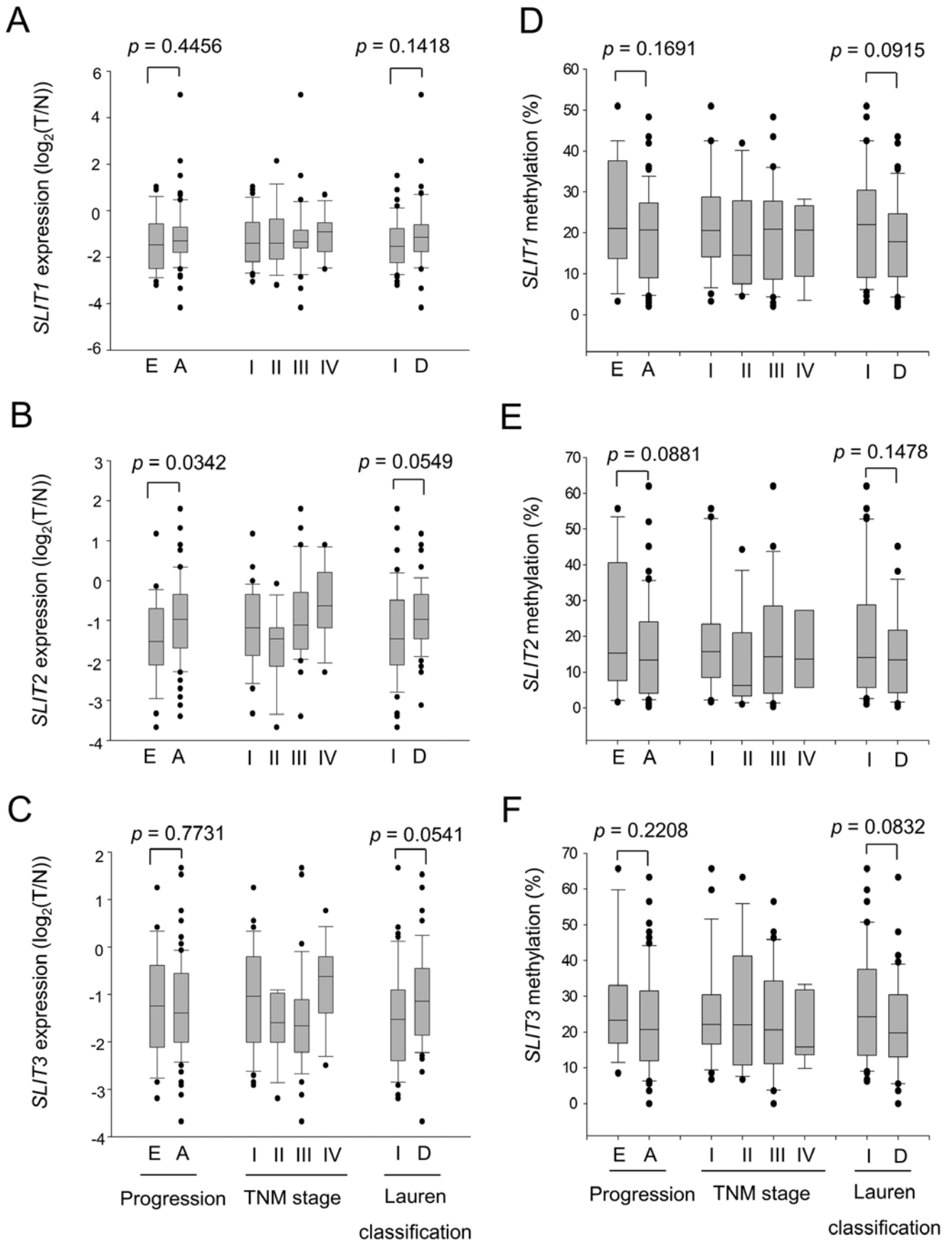


Figure 3. Expression and methylation of *SLIT* genes in gastric tumors. The expression of *SLIT1* (A), *SLIT2* (B), and *SLIT3* (C) in 96 pairs of normal and tumor tissues was measured by qRT-PCR and is expressed as the  $\log_2$  ratio of tumor over normal.  $\beta$ -actin was used as a control. Expression status was stratified by tumor progression (E, early; A, advanced), TNM stage (I, II, III, and IV), and Lauren classification (I, intestinal; D, diffuse). The methylation of promoter regions of *SLIT1* (D), *SLIT2* (E), and *SLIT3* (F) in 83 pairs of normal and tumor tissues was measured by pyrosequencing. Methylation status was stratified by tumor progression, TNM stage, and Lauren classification. Each box plot shows the median and 25th and 75th percentiles, and the dots represent outliers.

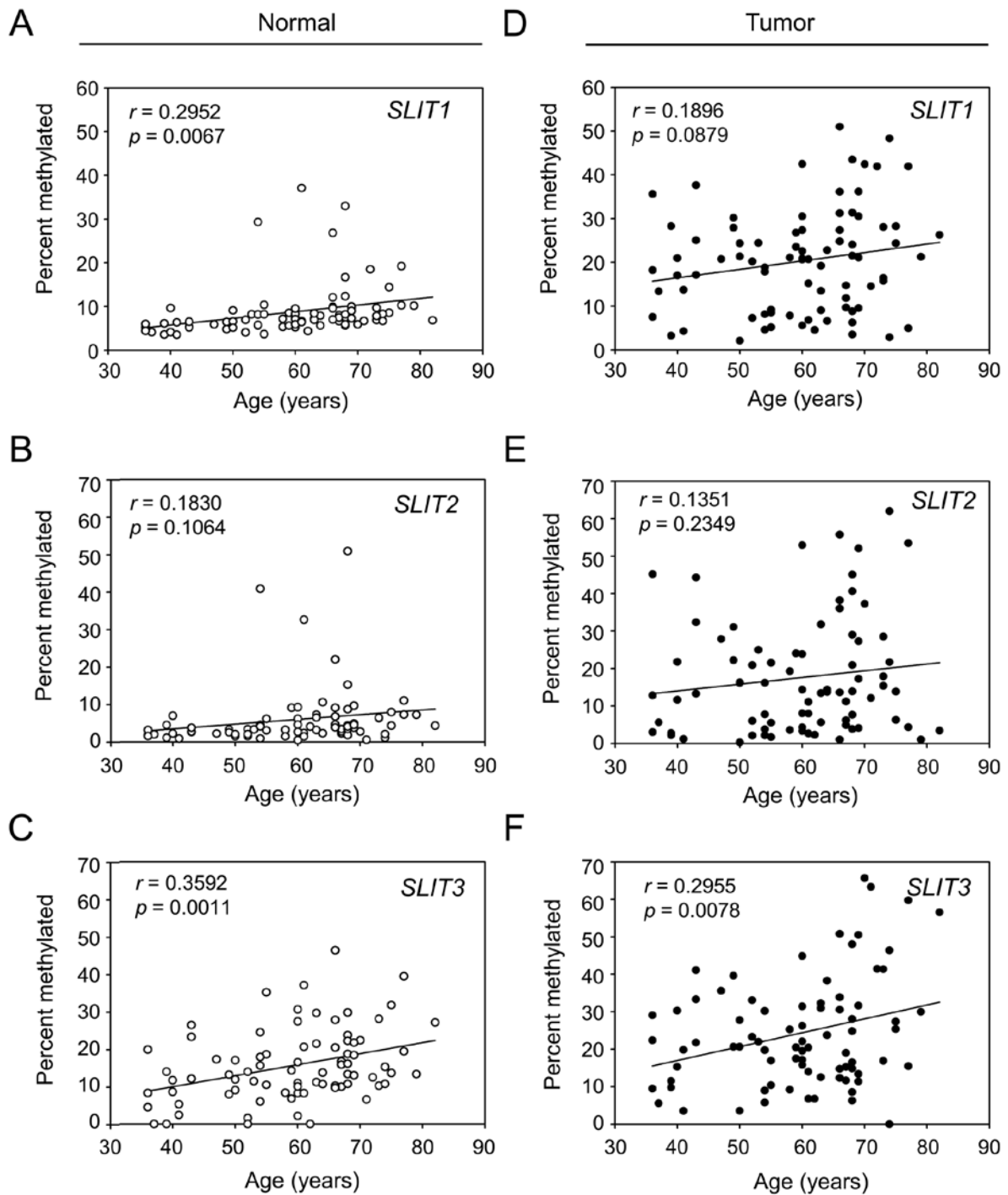


Figure 4. Hypermethylation of *SLIT* genes with patient age. Regression analysis of *SLIT1* (A and D), *SLIT2* (B and E), and *SLIT3* (C and F) methylation in gastric tumor and adjacent normal tissues according to patient age. Each methylation value from Fig. 2B for each sample was plotted against age. Open circles, normal tissues; filled circles, gastric tumors. Hypermethylation of *SLIT* genes increases with patient age. The regression coefficient and probability are given in each panel.

As expected from the high methylation levels of *SLIT* promoters in the EBV and MSI subtypes, these two subtypes had lower *SLIT* expression than the other subtypes (Fig. 6). Interestingly, expression of *SLIT2* and *SLIT3* was significantly increased in the GS subtype (Fig. 6B; *SLIT2*,  $p=0.0062$ , Fig. 6C; *SLIT3*,  $p=0.0027$ ). The CIN subtype had *SLIT* expression levels similar to those of normal gastric tissue (Fig. 6). These data suggested that epigenetic inactivation of *SLITs* occurs in a subtype-specific manner in gastric cancer.

*Downregulation of miR-218 through methylation of SLIT2 and SLIT3 CpG islands.* miR-218 is the mature form of miR-218-1 and miR-218-2, the intronic miRNAs that share the same promoter with their host gene transcripts, *SLIT2* and *SLIT3*, respectively (15). miRNA-seq of patient-derived gastric cancer cells and adjacent normal gastric mucosa cells showed that expression of miR-218-1 and miR-218-2 was silenced in gastric cancer cells (Fig. 7A and B). To examine the relationship between miR-218-1 and miR-218-2 expression and

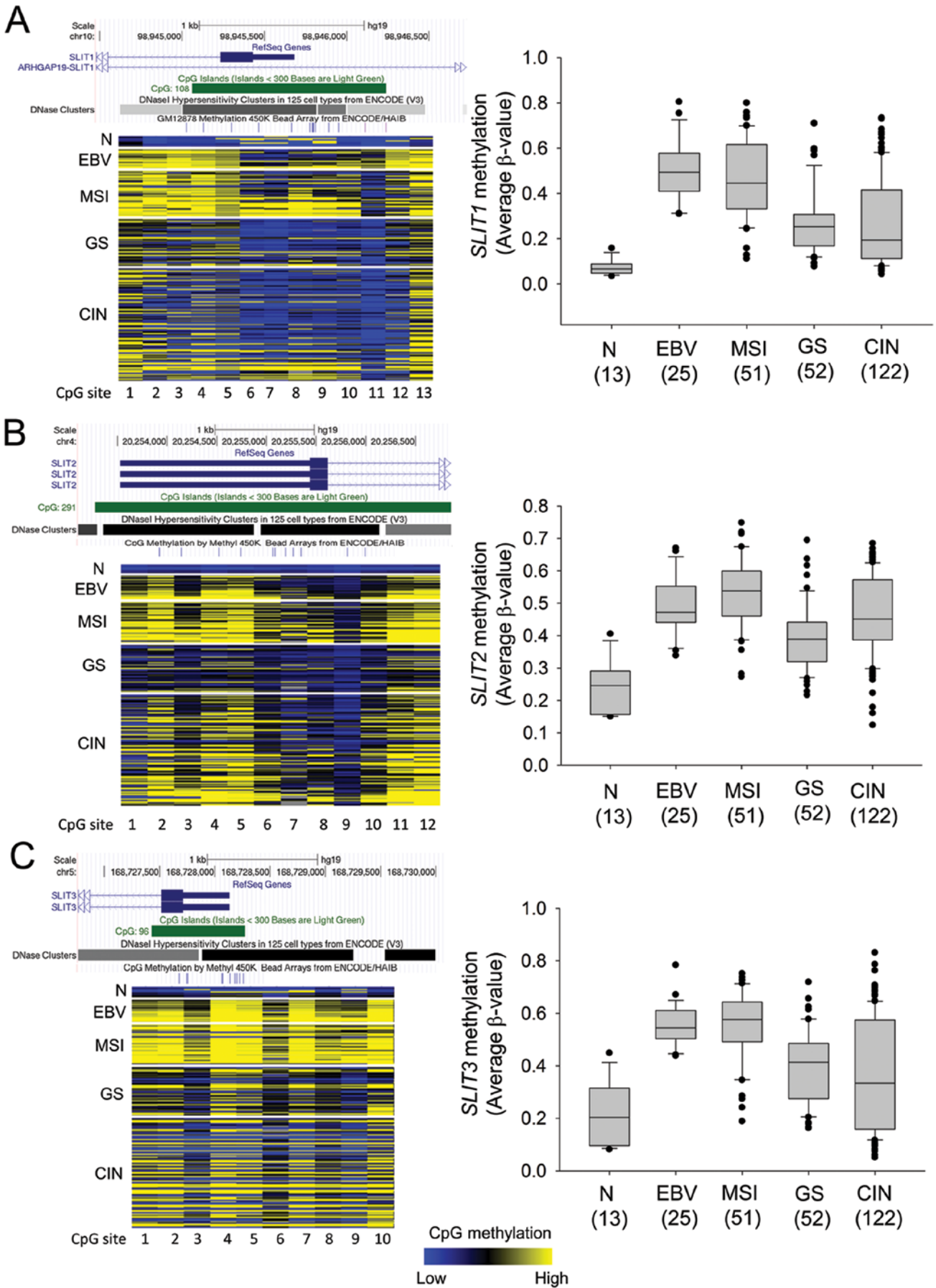


Figure 5. Methylation of *SLITs* in gastric cancer subtypes. Methylation of *SLIT1* (A), *SLIT2* (B), and *SLIT3* (C) in normal gastric tissues (N) and EBV, MSI, GS, and CIN subtypes of gastric cancer tissues. The Infinium 450K methylation array data for gastric cancer was provided by TCGA (2). A snapshot of the UCSC genome browser (<http://genome.ucsc.edu/>, hg19) shows the locations of CpG sites analyzed in this study. The heatmaps show the methylation status of each CpG site in each tissue sample. Box plots show the median and 25th and 75th percentiles, and the dots represent outliers.

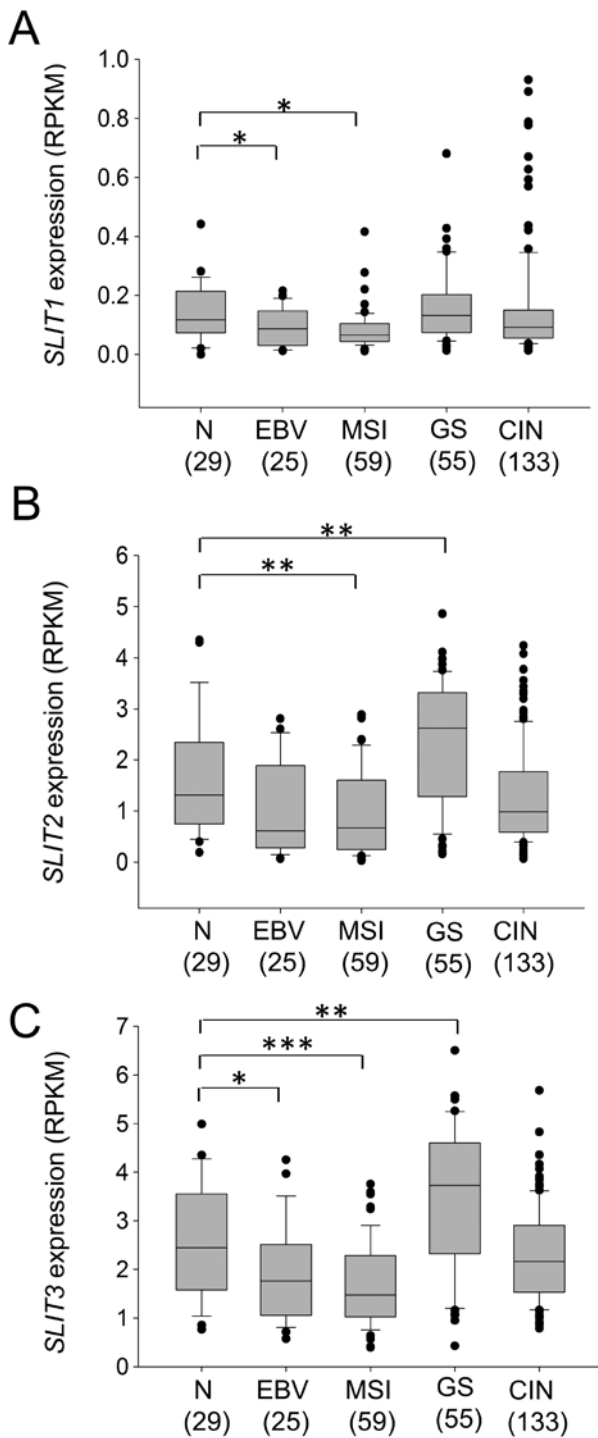


Figure 6. Expression of *SLITs* in gastric cancer subtypes. Expression of *SLIT1* (A), *SLIT2* (B), and *SLIT3* (C) in normal gastric tissues (N) and EBV, MSI, GS, and CIN subtypes of gastric cancer tissues. RNA-seq data for gastric cancer was provided by TCGA (2). Box plots show the median and 25th and 75th percentiles, and the dots represent outliers. \* $p < 0.05$ , \*\* $p < 0.01$ , \*\*\* $p < 0.001$ . RPKM, reads per kilobase per million.

CpG island methylation of *SLIT2* and *SLIT3*, we performed regression analysis using TCGA data. Decreasing miR-218-1 and miR-218-2 expression correlated with increasing CpG methylation of *SLIT2* ( $r = -0.4070$ ,  $p = 1 \times 10^{-10}$ ) and *SLIT3* ( $r = -0.2702$ ,  $p = 3 \times 10^{-5}$ ), respectively (Fig. 7C and D).

The expression of miR-218-2 was higher than that of miR-218-1 in both gastric normal and tumor tissues (Fig. 7E

and F). miR-218-2 expression was lower in EBV, MSI, and CIN subtypes (Fig. 7F), whereas miR-218-1 expression was lower in MSI (Fig. 7E). These data suggested that mature miR-218 is mainly derived from miR-218-2 in gastric cancer, and CpG island methylation of *SLIT3* reduces miR-218 expression in EBV, MSI, and CIN subtypes of gastric cancer.

## Discussion

Recent studies indicated that the SLIT/ROBO pathway has important roles in tumorigenesis, cancer progression, and metastasis (8,9). Furthermore, large-scale genomic studies discovered frequent mutations in SLIT/ROBO pathway genes in gastric cancer (26), pancreatic cancer (27), and small-cell lung cancer (28). These studies suggest that the SLIT/ROBO pathway is a master regulator for multiple oncogenic signaling pathways and a promising target for cancer therapy (8,9).

A methylation analysis of *SLIT* genes was previously performed using only a few cancer cell lines and primary tumor tissue samples (12,13). In this study, we analyzed expression and methylation of *SLITs* in 11 gastric cancer cell lines, 96 paired gastric tumors and adjacent normal gastric tissues, and 250 gastric cancers provided by TCGA (2). We found that all three *SLIT* genes were hypermethylated and downregulated at early stages of gastric cancer (Fig. 3), and hypermethylation was even detected in normal gastric tissues (Fig. 4). Interestingly, methylation of *SLIT1* and *SLIT3* correlated significantly with age in normal tissues (Fig. 4A and C). These results suggest that loss of *SLIT* expression is an early event in gastric cancer progression.

*SLITs* showed subtype-specific expression and methylation. Inactivation of *SLITs* by CpG island methylation mainly occurred in the EBV and MSI subtypes (Figs. 5 and 6). Interestingly, the GS subtype showed significantly increased expression of *SLIT2* and *SLIT3* (Fig. 6B and C). The GS subtype is considered as an aggressive, invasive, and stem-like gastric cancer. Therefore, this result supports the idea that the SLIT/ROBO pathway might inhibit cancer cell migration from the primary site. However, in metastatic tumors, the SLIT/ROBO system might increase cancer cell motility (9). More basic research is required to better understand the complex functions of these proteins during tumor progression.

The expression of miR-218 is significantly repressed in gastric, colon, prostate, and pancreatic cancers (15). miR-218 suppresses cancer progression by targeting the mRNAs encoding survivin (17), HOXB3 (29), Bmi1 (30), and components of the AKT/mTOR, SLIT/ROBO, Wnt, and focal adhesion pathways (15). In this study, we found that expression of miR-218-1 and miR-218-2 correlated negatively with CpG island methylation in *SLIT2* and *SLIT3*, respectively (Fig. 7). According to the expression pattern of their host genes, miR-218-1 and miR-218-2 were expressed in a gastric cancer subtype-specific manner. In particular, miR-218-2 expression was significantly reduced in the EBV and MSI subtypes (Fig. 7F). However, miR-218 expression in the GS subtype did not differ significantly from that in normal tissue. We therefore propose a subtype-specific role for miR-218 in gastric cancer.

In conclusion, we demonstrated that methylation of CpG islands inactivated *SLIT1*, *SLIT2* and *SLIT3* during early gastric tumor progression. *SLITs* were hypermethylated

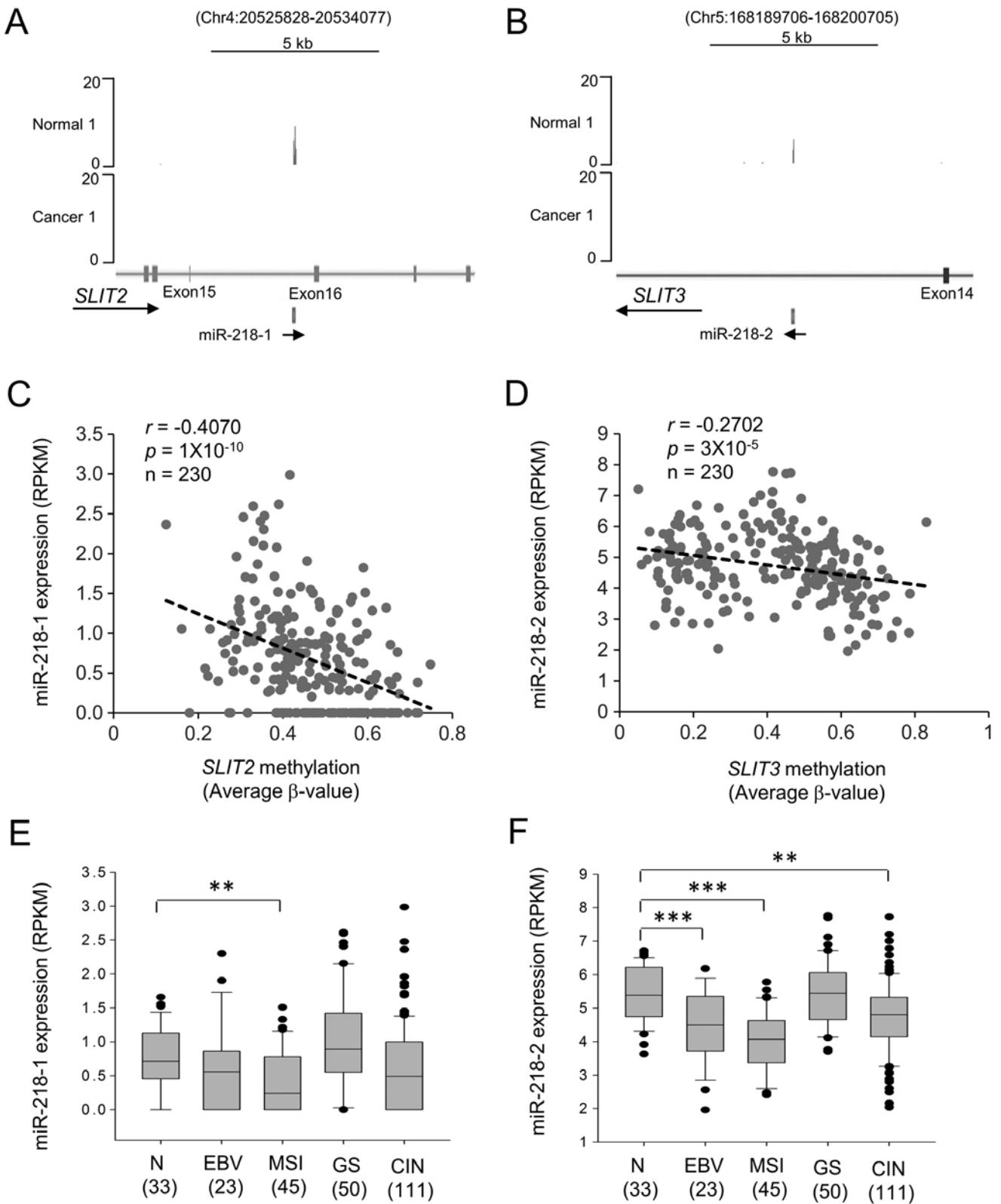


Figure 7. Expression of miR-218-1 and miR-218-2 in gastric cancer. miRNA-seq data for miR-218-1 (A) and miR-218-2 (B) in patient-derived gastric cancer cells and adjacent normal gastric mucosa cells. Relationship between miR-218-1 expression and *SLIT2* methylation (C) and miR-218-2 expression and *SLIT3* methylation (D). Expression of miR-218-1 (E) and miR-218-2 (F) in normal gastric tissues (N) and EBV, MSI, GS, and CIN subtypes of gastric cancer tissues. Box plots show the median and 25th and 75th percentiles, and the dots represent outliers. \* $p < 0.05$ , \*\* $p < 0.01$ , \*\*\* $p < 0.001$ . RPKM, reads per kilobase per million.

and downregulated in the EBV and MSI subtypes of gastric cancer, whereas *SLIT2* and *SLIT3* expression increased in the GS subtype. We also showed that miR-218-1 and miR-218-2

expression correlated negatively with CpG island methylation in *SLIT2* and *SLIT3*, respectively. Although more basic research should be conducted to understand the subtype-specific roles

of SLITs and miR-218, we suggest that a subtype-specific therapeutic strategy targeting SLITs and miR-218 should be considered for treatment of gastric cancer.

### Acknowledgements

This study was supported by National Research Foundation of Korea (NRF) grants funded by the Korea government (NRF-2012M3A9B4027954 and NRF-2013R1A1A2006621) and a KRIBB research initiative grant.

### References

- Lauren P: The two histological main types of gastric carcinoma: Diffuse and so-called intestinal-type carcinoma. An attempt at a histo-clinical classification. *Acta Pathol Microbiol Scand* 64: 31-49, 1965.
- Bass AJ, Thorsson V, Shmulevich I, Reynolds SM, Miller M, Bernard B, Hinoue T, Laird PW, Curtis C, Shen H, *et al*: Cancer Genome Atlas Research Network: Comprehensive molecular characterization of gastric adenocarcinoma. *Nature* 513: 202-209, 2014.
- Fukayama M, Hino R and Uozaki H: Epstein-Barr virus and gastric carcinoma: Virus-host interactions leading to carcinoma. *Cancer Sci* 99: 1726-1733, 2008.
- Kaneda A, Matsusaka K, Aburatani H and Fukayama M: Epstein-Barr virus infection as an epigenetic driver of tumorigenesis. *Cancer Res* 72: 3445-3450, 2012.
- Velho S, Fernandes MS, Leite M, Figueiredo C and Seruca R: Causes and consequences of microsatellite instability in gastric carcinogenesis. *World J Gastroenterol* 20: 16433-16442, 2014.
- Yamamoto H, Watanabe Y, Maehata T, Morita R, Yoshida Y, Oikawa R, Ishigooka S, Ozawa S, Matsuo Y, Hosoya K, *et al*: An updated review of gastric cancer in the next-generation sequencing era: Insights from bench to bedside and vice versa. *World J Gastroenterol* 20: 3927-3937, 2014.
- Kidd T, Bland KS and Goodman CS: Slit is the midline repellent for the robo receptor in *Drosophila*. *Cell* 96: 785-794, 1999.
- Gara RK, Kumari S, Ganju A, Yallapu MM, Jaggi M and Chauhan SC: Slit/Robo pathway: A promising therapeutic target for cancer. *Drug Discov Today* 20: 156-164, 2015.
- Mehlen P, Delloye-Bourgeois C and Chédotal A: Novel roles for Slits and netrins: Axon guidance cues as anticancer targets? *Nat Rev Cancer* 11: 188-197, 2011.
- Prasad A, Paruchuri V, Preet A, Latif F and Ganju RK: Slit-2 induces a tumor-suppressive effect by regulating beta-catenin in breast cancer cells. *J Biol Chem* 283: 26624-26633, 2008.
- Shi R, Yang Z, Liu W, Liu B, Xu Z and Zhang Z: Knockdown of Slit2 promotes growth and motility in gastric cancer cells via activation of AKT/ $\beta$ -catenin. *Oncol Rep* 31: 812-818, 2014.
- Dallol A, Da Silva NF, Viacava P, Minna JD, Bieche I, Maher ER and Latif F: SLIT2, a human homologue of the *Drosophila* Slit2 gene, has tumor suppressor activity and is frequently inactivated in lung and breast cancers. *Cancer Res* 62: 5874-5880, 2002.
- Dickinson RE, Dallol A, Bieche I, Krex D, Morton D, Maher ER and Latif F: Epigenetic inactivation of SLIT3 and SLIT1 genes in human cancers. *Br J Cancer* 91: 2071-2078, 2004.
- Narayan G, Goparaju C, Arias-Pulido H, Kaufmann AM, Schneider A, Dürst M, Mansukhani M, Pothuri B and Murty VV: Promoter hypermethylation-mediated inactivation of multiple Slit-Robo pathway genes in cervical cancer progression. *Mol Cancer* 5: 16, 2006.
- Lu YF, Zhang L, Waye MM, Fu WM and Zhang JF: MiR-218 mediates tumorigenesis and metastasis: Perspectives and implications. *Exp Cell Res* 334: 173-182, 2015.
- Tatarano S, Chiyomaru T, Kawakami K, Enokida H, Yoshino H, Hidaka H, Yamasaki T, Kawahara K, Nishiyama K, Seki N, *et al*: miR-218 on the genomic loss region of chromosome 4p15.31 functions as a tumor suppressor in bladder cancer. *Int J Oncol* 39: 13-21, 2011.
- Alajez NM, Lenarduzzi M, Ito E, Hui AB, Shi W, Bruce J, Yue S, Huang SH, Xu W, Waldron J, *et al*: MiR-218 suppresses nasopharyngeal cancer progression through downregulation of survivin and the SLIT2-ROBO1 pathway. *Cancer Res* 71: 2381-2391, 2011.
- Tie J, Pan Y, Zhao L, Wu K, Liu J, Sun S, Guo X, Wang B, Gang Y, Zhang Y, *et al*: MiR-218 inhibits invasion and metastasis of gastric cancer by targeting the Robo1 receptor. *PLoS Genet* 6: e1000879, 2010.
- Kim M, Kim JH, Jang HR, Kim HM, Lee CW, Noh SM, Song KS, Cho JS, Jeong HY, Hahn Y, *et al*: LRRC3B, encoding a leucine-rich repeat-containing protein, is a putative tumor suppressor gene in gastric cancer. *Cancer Res* 68: 7147-7155, 2008.
- Kim M, Park YK, Kang TW, Lee SH, Rhee YH, Park JL, Kim HJ, Lee D, Lee D, Kim SY, *et al*: Dynamic changes in DNA methylation and hydroxymethylation when hES cells undergo differentiation toward a neuronal lineage. *Hum Mol Genet* 23: 657-667, 2014.
- Haam K, Kim HJ, Lee KT, Kim JH, Kim M, Kim SY, Noh SM, Song KS and Kim YS: Epigenetic silencing of BTB and CNC homology 2 and concerted promoter CpG methylation in gastric cancer. *Cancer Lett* 351: 206-214, 2014.
- Kim SK, Jang HR, Kim JH, Kim M, Noh SM, Song KS, Kang GH, Kim HJ, Kim SY, Yoo HS, *et al*: CpG methylation in exon 1 of transcription factor 4 increases with age in normal gastric mucosa and is associated with gene silencing in intestinal-type gastric cancers. *Carcinogenesis* 29: 1623-1631, 2008.
- Jones PA and Taylor SM: Cellular differentiation, cytidine analogs and DNA methylation. *Cell* 20: 85-93, 1980.
- Lokk K, Modhukur V, Rajashekar B, Märten K, Mägi R, Kolde R, Koltšina M, Nilsson TK, Vilo J, Salumets A, *et al*: DNA methylome profiling of human tissues identifies global and tissue-specific methylation patterns. *Genome Biol* 15: r54, 2014.
- Nazor KL, Altun G, Lynch C, Tran H, Harness JV, Slavin I, Garitaonandia I, Müller FJ, Wang YC, Boscolo FS, *et al*: Recurrent variations in DNA methylation in human pluripotent stem cells and their differentiated derivatives. *Cell Stem Cell* 10: 620-634, 2012.
- Wong SS, Kim KM, Ting JC, Yu K, Fu J, Liu S, Cristescu R, Nebozhyn M, Gong L, Yue YG, *et al*: Genomic landscape and genetic heterogeneity in gastric adenocarcinoma revealed by whole-genome sequencing. *Nat Commun* 5: 5477, 2014.
- Biankin AV, Waddell N, Kassahn KS, Gingras MC, Muthuswamy LB, Johns AL, Miller DK, Wilson PJ, Patch AM, Wu J, *et al*: Australian Pancreatic Cancer Genome Initiative: Pancreatic cancer genomes reveal aberrations in axon guidance pathway genes. *Nature* 491: 399-405, 2012.
- Peifer M, Fernández-Cuesta L, Sos ML, George J, Seidel D, Kasper LH, Plenker D, Leenders F, Sun R, Zander T, *et al*: Integrative genome analyses identify key somatic driver mutations of small-cell lung cancer. *Nat Genet* 44: 1104-1110, 2012.
- Li Q, Zhu F and Chen P: miR-7 and miR-218 epigenetically control tumor suppressor genes RASSF1A and Claudin-6 by targeting HoxB3 in breast cancer. *Biochem Biophys Res Commun* 424: 28-33, 2012.
- Tu Y, Gao X, Li G, Fu H, Cui D, Liu H, Jin W and Zhang Y: MicroRNA-218 inhibits glioma invasion, migration, proliferation, and cancer stem-like cell self-renewal by targeting the polycomb group gene Bmi1. *Cancer Res* 73: 6046-6055, 2013.